ELSEVIER

Journal of Photochemistry and Photobiology A: Chemistry 150 (2002) 101–108

Journal of Photochemistry and Photobiology A:Chemistry

www.elsevier.com/locate/jphotochem

Long-lived photoinduced charge separation in carbazole–pyrene–viologen system incorporated in Langmuir–Blodgett films of substituted diazacrown ethers

Jiu-Yan Li, Ming-Li Peng, Li-Ping Zhang, Li-Zhu Wu, Bo-Jie Wang, Chen-Ho Tung*

Technical Institute of Physics and Chemistry, Chinese Academy of Sciences, Beijing 100101, PR China

Received 22 August 2001; received in revised form 5 February 2002; accepted 11 March 2002

Abstract

Diaza-18-crown-6 ethers appending two pyrenyl (Py) or two carbazolyl (Cz) groups were synthesized. These macrocyclic compounds form 1:1 host–guest complexes with methyl viologen chloride (MV^{2+}), and these complexes were assembled into monolayers by Langmuir–Blodgett technique. The generated assembly involves the general structure of donor–sensitizer–acceptor (Cz–Py–MV^{2+}) in space, although any of the photo- and redox-active components are not covalently bonded. Photoirradiation of the pyrenyl group resulted in the charge-separated pair $Cz^{\bullet+}$–Py–$MV^{\bullet+}$ which survived up to hours in a well anaerobic atmosphere. An electrode was fabricated by transferring the L–B film on an ITO glass. The photoinduced voltage of this electrode was measured with a saturated calomel reference electrode in hydroquinone (H_2Q) solution to be ca. 168 mV when the light intensity was 218 mW/cm^2. This electrode was also used as the light electrode to construct a photogalvanic cell with a platinum electrode as the dark electrode. Irradiation of the light electrode with visible light results in anodic photocurrent, and there is no net chemical change associated with the function of the cell which converts light to electricity. © 2002 Published by Elsevier Science B.V.

Keywords: Photoinduced charge separation; Carbazole–pyrene–viologen; Langmuir–Blodgett films; Diazacrown ethers

1. Introduction

Photoinduced electron transfer and the subsequent charge separation are principle stages in photoconversion of solar energy into chemical or electric energy [1–3]. An efficient photoconversion system would have unity quantum efficiency for electron transfer and would yield charge separation states that did not back electron transfer. In fact, these ideal requirements are highly unrealistic since often the means to attain one goal is the direct opposite of the means to attain another [4]. Thus, for efficient forward electron transfer, the distance between the donor and the acceptor should be short. On the other hand, only if the charges generated by forward electron transfer are in a large distance, the energy-wasting back electron transfer can be effectively impeded. Nevertheless, the natural photosynthetic reaction center does achieve a high quantum efficiency for charge separation without losses from back electron transfer. This has been attained via an evolutionarily optimized, fixed spatial arrangement of functional molecular compounds which, through a sequence of fast short-distance electron transfers, separate charge to large distance and thus avoid the energy-dissipating back electron transfer. This principle of optimized photoinduced charge separation through a series of small distance charge transfer steps (rather than a long-distance single-step reaction) has been applied to the design of many artificial photosynthesis systems. Two basic approaches to the organizing component molecules in space have emerged [5]. One is to synthesize supermolecules, in which the order and spacing of subunits in a chain is fixed by covalent bonds [6–9]. Although the system obtained by this method is quite effective for light energy photoconversion, the synthesis becomes increasingly demanding as more chromophores and redox-active units are added. Another strategy is to use supramolecular supports or self-assembling systems [10–20]. In this case the synthesis is easier, but it is hard to attain the required high efficiency for light energy conversion. A combined approach in which relatively small supermolecules (diads and triads) are organized into a larger self-assembling system, is also possible.

In this paper, we describe the construction of a donor (D)–sensitizer (S)–acceptor (A) system by Langmuir–Blodgett technique, which can perform sequential electron transfer reactions. We use carbazolyl and pyrenyl, each of

* Corresponding author. Tel.: +86-10-6488-8046; fax: +86-10-6487-9375.
E-mail address: chtung@ipc.ac.cn (C.-H. Tung).

1010-6030/02/$ – see front matter © 2002 Published by Elsevier Science B.V.
PII: S1010-6030(02)00133-8

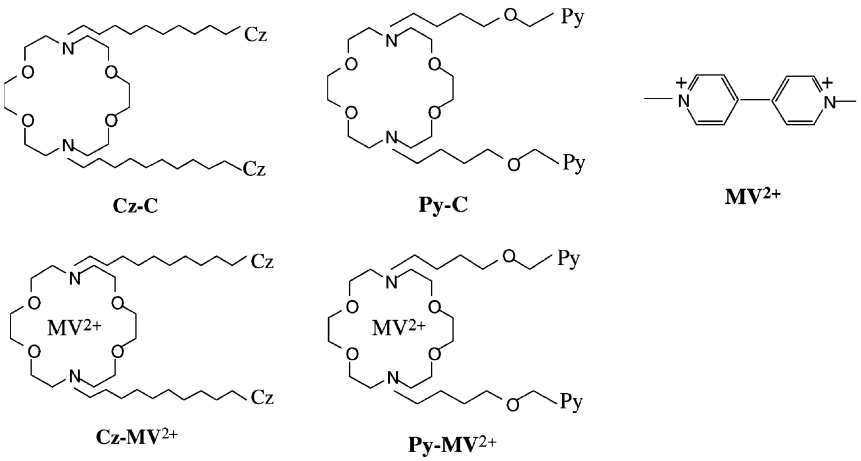

Scheme 1.

which is covalently connected to a diazacrown ether ring, as the electron donor and sensitizer, respectively, and make them form complexes with an electron acceptor methyl viologen chloride (MV^{2+}) via the crown ether moieties. Then, these complexes as building blocks are assembled into a film by L–B technique. As shown in Scheme 1, each diazacrown ether moiety has appended either two carbazolyl through $(CH_2)_{10}$ or two pyrenyl through $CH_2O(CH_2)_4$ groups to constitute Cz–C or Py–C. If their complexes with MV^{2+} (Cz–MV^{2+} and Py–MV^{2+}) are assembled in a molar ratio of 1:1, the ratio of D:S:A moieties would be 1:1:1. Thus this system involve the general structure of D–S–A in space, in which there are no covalent bonds between any of the photo- or redox-active components. The short distance between D and S, and between S and A leads to fast forward electron transfer, and the spatial separation between the donor and the acceptor inhibits the back electron transfer. An exceedingly long-lived (up to hours) charge separation pair was achieved. Furthermore, a photoelectrochemical cell constructed on the basis of the above system displays the function of conversion of light to electricity.

2. Experiment

2.1. Materials and instruments

Methyl viologen chloride (MV^{2+}) was Aldrich product and used directly without further purification. Stearic acid (SA) and methanol were spectra-grade and were used for preparation of L–B films and for absorption and emission spectrum measurements, respectively. Water used as subphase was deionized and distilled three times. Pyrenyl and carbazolyl appended diazacrown ethers (Py–C and Cz–C) were synthesized by two steps: reaction of triethylene glycol with 1,2-bis(2-aminoethoxy)ethane yielded 1,7,10,16-tetraoxo-4,13-diazacyclooctadecane (diaza-18-crown-6) [21] with a yield of 30%. This crown ether reacted, respectively, with 1-(4-bromobutoxymethyl)pyrene and *N*-(10-bromodecyl)carbazole to give Py–C and Cz–C. The details of the syntheses for these compounds are given in Appendix A.

Absorption spectra were recorded on a PE Lambda 20 UV–Vis spectrometer. Fluorescence spectra were measured on a PE LS 50B luminescence spectrometer. In irradiation experiments of solution, a xenon lamp was applied as the light source and acetone was used as a filter to cut off the light with $\lambda < 330$ nm. The L–B films were prepared by a Joyce Loebl Langmuir Trough 4 machine. AFM measurements were performed on a Digital Instruments Nanoscope III Multimode system (Santa Barbara, CA) with a 160 μm scanner in the Tapping mode. The photoelectrochemical studies were performed by using a model 600 voltametry analyzer (CH Instruments, USA).

2.2. Redox potential and complexation constant measurements

The redox potential of MV^{2+} in its complex with Py–C or Cz–C were determined by cyclic voltammetry in acetonitrile using a glassy carbon working electrode and an Ag/AgCl/KCl (saturated) reference electrode in the presence of 0.1 M tetrabutylammonium hexafluorophosphate as the supporting electrolyte.

The complexation constant between Cz–C (or Py–C) and MV^{2+} was determined by measurement of the fluorescence intensities of Cz–C in methanol at constant Cz–C concentration and various MV^{2+} concentrations. The data were analyzed by the Hildebrand–Benesi expression [22]

$$\frac{1}{I - I_0} = \frac{1}{\alpha[\text{Cz–C}]} + \left\{\frac{1}{\alpha[\text{Cz–C}]K}\right\}\left(\frac{1}{[MV^{2+}]}\right) \quad (1)$$

where I_0 and I are the fluorescence intensities of Cz–C in methanol in the absence and presence of MV^{2+}, respectively; K the complexation constant. At concentrations of MV^{2+} below 5×10^{-6} M, the plot of $1/(I - I_0)$ as a function

of 1/[MV^{2+}] is linear, strongly suggesting the formation of 1:1 complex between Cz–C and MV^{2+}. Analysis of the plot gives the *K* value.

2.3. Preparation of L–B films

A solution of Py–MV^{2+} (5×10^{-4} M) and SA (molar ratio = 1:2) in the mixed solvent of chloroform and methanol (9:1 in vol.%) was spread onto a distilled water subphase at a subphase temperature of $25 \pm 1\,^{\circ}C$. The solvents were allowed to evaporate for 15 min, and the floating film was then compressed at a rate of 0.8 cm^2/min. The substrate monolayer was transferred on an ITO-coated glass under a constant surface pressure of 25 mN/cm^2. The thickness of the L–B film was measured by AFM technique. Similarly, the L–B film of Cz–MV^{2+}, and that of the mixture of Py–MV^{2+} and Cz–MV^{2+} were prepared.

2.4. Absorption and fluorescence measurements

The L–B film on quartz glass substrate was placed in a quartz cell equipped with a vacuum stopcock. The sample was degassed thoroughly (10^{-4} mm Hg) and the cell was sealed. Fluorescence quenching of Py and Cz by MV^{2+}, and the absorption of the generated viologen radical $MV^{\bullet+}$ in the L–B films were measured at room temperature. The excitation wavelengths for the fluorescence quenching study of Py and Cz were 345 and 295 nm, respectively. The relative fluorescence efficiencies were measured from the peak areas of the fluorescence spectra.

2.5. Photoelectrochemical measurements

An ITO-coated electrode was coated with an L–B film containing Py–MV^{2+} and Cz–MV^{2+}. The measurements of photovoltage were conducted with a saturated calomel reference electrode in 36 mM hydroquinone (H_2Q) aqueous solution, while those of photocurrent with a platinum counter electrode in aqueous solution containing 36 mM H_2Q and 0.1 M KCl. Irradiation of the cell was performed by a 500 W xenon lamp. The light intensity was ca. 218 mW/cm^2. The voltage and current changes induced by switching on and off the light were recorded. The current direction was expressed based on the ITO electrode as the working electrode.

3. Results and discussion

3.1. Electron transfer from excited states of pyrenyl and carbazolyl to methyl viologen in L–B films

It has been well established [23–26] that macrocyclic crown ethers such as diaza-18-crown-6 ether can form 1:1 host–guest complexes with MV^{2+}. We prepared the complex of Py–C with MV^{2+} (Py–MV^{2+}) simply by mixing these two components in methanol. By measurement of the fluorescence intensities of Py–C at constant Py–C concentration and various MV^{2+} concentrations and analysis of the data according to the Hildebrand–Benesi equation [22], we demonstrated that these two components indeed form 1:1 host–guest complex (Section 2). The complexation constant was estimated to be ca. 1.5×10^2 M^{-1}. During the experiments, no release of MV^{2+} from the complex was observed. This complex in the presence of SA can be easily assembled into a film by L–B technique. Curve 1 in Fig. 1 shows the typical surface pressure–area (π–*A*) isotherm for a mixture of Py–MV^{2+} and SA with the molar ratio of 1:2. The limiting area per Py–MV^{2+} molecule is ca. 150 $Å^2$ obtained by extrapolating the curve under 25 mN/m. This value is comparable with that of the molecule area of the diaza-18-crown-6 ether 144 $Å^2$ which is obtained by PCMODEL program calculation. This observation suggests that the molecular plain of the crown ether parallelizes the air–water interface, and the methyl viologen molecule does not occupy an extra area in the monolayer, instead it just locates (at least partially) in the crown ether cavity of Py–C. Stability experiments for the monolayer exhibit that the limiting area keeps constant for at least half an hour under the surface pressure of 25 mN/cm^2. Thus a stable and condensed monolayer was formed. The film was successfully transferred onto an ITO glass substrate with a typical transfer ratio of 0.95 ± 0.05, and examined by AFM on a Digital Instruments Nanoscope III Multimode system (Santa Barbara, CA) with a 160 μm scanner in the Tapping mode. The results show that the film is uniform and the thickness of the Py–MV^{2+} monolayer is ca. 2.5 nm. This value corresponds to the length of Py–MV^{2+} molecule assuming that the spacer chain is in an extended conformation and the molecular plain of the crown ether complexing MV^{2+} is vertical to the chain. Thus, we proposed that the side arm chains in Py–MV^{2+} film are oriented to be vertical to the substrate surface.

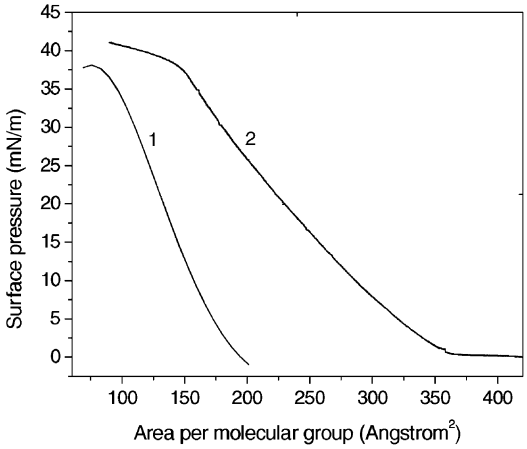

Fig. 1. Surface pressure–area isotherms of Py–MV^{2+} with SA (molar ratio = 1:2) (curve 1), and the mixture of Py–MV^{2+} and Cz–MV^{2+} with SA (molar ratio = 1:1:2) (curve 2) at the air–water interface (25 °C). The limiting area per Py–MV^{2+} molecule is ca. 150 $Å^2$, and the limiting area per pair of Py–MV^{2+} and Cz–MV^{2+} molecule is ca. 300 $Å^2$.

Similarly, the L–B film of the mixture of Py–C and SA with molar ratio of 1:2 (in the absence of MV^{2+}) on a glass substrate was also fabricated. The L–B films of Py–MV^{2+} and Py–C were thoroughly vacuumed in a quartz cell, and the fluorescence intensity was measured at the excitation wavelength of 345 nm. While Py–C on L–B film shows strong fluorescence of pyrenyl excimer and monomer with the former dominating the emission spectrum, the fluorescence of the pyrenyl for Py–MV^{2+} on L–B film was totally quenched by the MV^{2+}. The energy of the singlet excited state of the pyrenyl is lower than that of MV^{2+} as estimated from their absorption spectra. Thus, the possibility of singlet–singlet energy transfer responsible for the fluorescence quenching is excluded. Therefore, we examined the reality of electron transfer between the two chromophores as the cause of the fluorescence quenching. The free energy change (ΔG) involved in a photostimulated electron transfer process can be estimated by Rehm–Weller equation [27–30]:

$$\Delta G = E_{ox}(D) - E_{red}(A) - \Delta E_{00} - \frac{e^2}{\varepsilon a} \quad (2)$$

where ΔE_{00} is the excited state energy, and in this case represents the singlet excited state energy of Py (ca. 77 kcal/mol) [31]. $E_{ox}(D)$ and $E_{red}(A)$ are the redox potentials of the donor and the acceptor, respectively, and in this case the oxidation potential of Py is ca. 1.20 V vs SCE [32] and the reduction potential of MV^{2+} in the complex were measured by cyclic voltammetry (Section 2) to be ca. −0.26 V vs SCE. $e^2/\varepsilon a$ is the Coulombic interaction in the ion pair state whose magnitude depends on the distance (a) between the donor and the acceptor and on the dielectric constant (ε) of the medium separating the charges [27–30]. For a contact ion pair in acetonitrile, this term is estimated to be ca. −0.05 V, and generally shows a minor impact on ΔG. Calculation according to Eq. (2) reveals that electron transfer from the singlet excited state of Py to MV^{2+} is exothermic by ca. −42 kcal/mol. The possibility of the electron transfer from Py excimer to MV^{2+} was also examined. Assuming the excitation energy of the excimer being ca. 59.6 kcal/mol (the λ_{max} of the excimer emission is ca. 480 nm), ΔG was calculated to be ca. −24.8 kcal/mol. Thus, we attributed the fluorescence quenching to the electron transfer from both the singlet excited state and the excimer of Py to MV^{2+}. The complete quenching of Py fluorescence by MV^{2+} suggests that the electron transfer process in Py–MV^{2+} L–B film effectively competes with the intrinsic decay processes of the singlet excited pyrenyl. The quenching rate constant is estimated to be greater than $4.4 \times 10^6\ s^{-1}$ based on the Py intrinsic fluorescence lifetime of 225 ns. The occurrence of the electron transfer between excited Py and MV^{2+} is supported by the observation of the absorption spectra of the generated viologen radical $MV^{\bullet+}$. Irradiation of the pyrenyl chromophore in Py–MV^{2+} L–B film with light $\lambda > 330$ nm in a thoroughly degassed quartz cell readily results in the absorption of $MV^{\bullet+}$ in two bands with λ_{max} at ca. 396 and 600 nm [33,34] as shown in Fig. 2. This charge separation

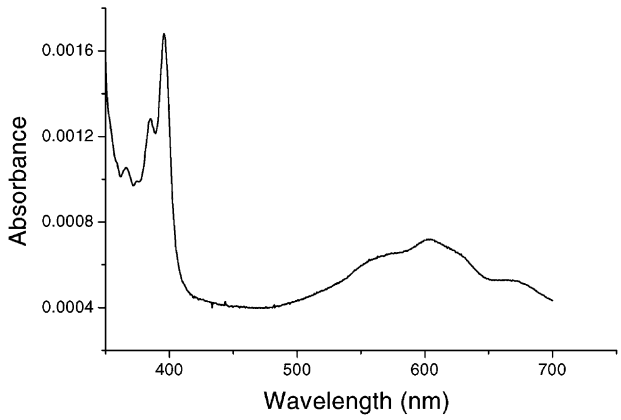

Fig. 2. Absorption spectrum of $MV^{\bullet+}$ radical in Py–MV^{2+} L–B film after irradiation of 30 s with $\lambda > 330$ nm light under an anaerobic atmosphere.

state may survive up to tens of minutes under anaerobic atmosphere.

Qualitatively similar results were obtained for the electron transfer from the excited state of carbazolyl to MV^{2+} in Cz–MV^{2+} L–B films. The L–B films of Cz–C and Cz–MV^{2+} were prepared in the presence of SA with the molar ratio of 1:2, and transferred to ITO glasses. AFM measurements show that the thickness of the L–B films is ca. 3.5 nm, corresponding to the length of Cz–MV^{2+} molecule assuming that the spacer chain is in an extended conformation and the molecular plain of the crown ether complexing MV^{2+} is vertical to the chain. The Cz chromophore in Cz–C L–B film in a thoroughly degassed cell shows structural monomer fluorescence with maxima at 357 and 372 nm and weak excimer fluorescence with maximum at 412 nm (excited at 295 nm). Under identical condition, this emission was quenched by MV^{2+} in Cz–MV^{2+} L–B film to ca. 30%. We believe that the quenching is due to electron transfer from the singlet excited Cz to MV^{2+}, since the calculated ΔG involved in this electron transfer process according to Eq. (2) is exothermic by ca. −50 kcal/mol, assuming that the energy of the carbazolyl singlet excited state is 83.2 kcal/mol [35], and the oxidation potential of Cz is ca. 1.10 V vs SCE [35]. Furthermore, irradiation of Cz–MV^{2+} L–B film in a thoroughly vacuumed cell resulted in $MV^{\bullet+}$ radical as detected by absorption spectrum. Obviously, the electron transfer in Cz–MV^{2+} L–B film is less efficient compared with that in Py–MV^{2+} L–B film. This observation is probably due to the larger donor–acceptor separation in Cz–MV^{2+} film (3.5 nm) than that in Py–MV^{2+} film (2.5 nm).

3.2. Photoinduced charge separation in Cz–Py–MV^{2+} L–B film

In the presence of SA, the mixture of Py–MV^{2+} and Cz–MV^{2+} can form well-organized L–B film. Curve 2 in Fig. 1 presents the π–A isotherm for the mixture of Py–MV^{2+}, Cz–MV^{2+} and SA with molar ratio of 1:1:2 at

the air–water interface. The average area occupied by per pair of Py–MV^{2+} and Cz–MV^{2+} molecules is ca. 300 $Å^2$, suggesting that the molecules of Py–MV^{2+} and Cz–MV^{2+} occupy the same surface area as in their respective L–B films. The thickness of the film is ca. 3.5 nm as measured by AFM technique. This value is identical to that of Cz–MV^{2+} L–B film, and corresponds to the length of Cz–MV^{2+} assuming that the spacer chain is in an extended conformation and the crown ether plain is vertical to the chain. All of these observations suggest that the side arm chains in the L–B film of the Cz–MV^{2+} and Py–MV^{2+} mixture are oriented to be vertical to the substrate surface. On the basis of the length of the linking chain in Py–MV^{2+} and Cz–MV^{2+}, we assume that the arrangement of the chromophores in space would be in a D–S–A (Cz–Py–MV^{2+}) sequence, although there are no covalent bonds between any of them. Absorption spectra show that at the wavelengths greater than 300 nm both pyrenyl and carbazolyl exhibit absorption, but no absorption for MV^{2+} is observed. The absorption of pyrenyl at this wavelength range is much stronger than that of carbazolyl. For example, at 345 nm for the solution with identical concentration, the absorption of pyrenyl is 10 times stronger than that of carbazolyl. Thus, at this wavelength mainly the pyrenyl moiety is excited, and the Cz–Py–MV^{2+} system acts like a D–S–A system. Irradiation of the L–B film in a thoroughly degassed quartz cell readily resulted in the generation of the charge separation state $Cz^{\bullet+}$–Py–$MV^{\bullet+}$ as detected by UV absorption of $MV^{\bullet+}$ radical, which can survive up to hours. Scheme 2 summarizes the charge separation processes. The singlet excited state of the pyrenyl (both monomer and excimer) in Cz–Py–MV^{2+} is readily quenched by MV^{2+} (process 1 in Scheme 2) as demonstrated above, generating Cz–$Py^{\bullet+}$–$MV^{\bullet+}$. The carbazolyl should easily transfer an electron to $Py^{\bullet+}$ (process 2 in Scheme 2) to form the charge separation state $Cz^{\bullet+}$–Py–$MV^{\bullet+}$, as the oxidation potential of carbazolyl (ca. 1.10 V vs SCE) [35] is less than that of pyrenyl (ca. 1.20 V vs SCE) [32]. Another possible path for the formation of the charge separation state $Cz^{\bullet+}$–Py–$MV^{\bullet+}$ involves electron transfer from the carbazolyl to the singlet excited state of the pyrenyl (process 3 in Scheme 2). Indeed, the ΔG involved in process 3 calculated by Eq. (2) is ca. −9.2 kcal/mol assuming that the energy of the excited state of pyrenyl is 77 kcal/mol and the reduction potential of pyrenyl is −1.79 V vs SCE [36]. Furthermore, in L–B film of the mixture of Py–C and Cz–C, the fluorescence of the pyrenyl is significantly quenched by the carbazolyl. Process 4 should also be exothermic as the reduction potential of the pyrenyl (−1.79 V vs SCE) [36] is much greater than that of MV^{2+} in its complex (−0.26 V vs SCE).

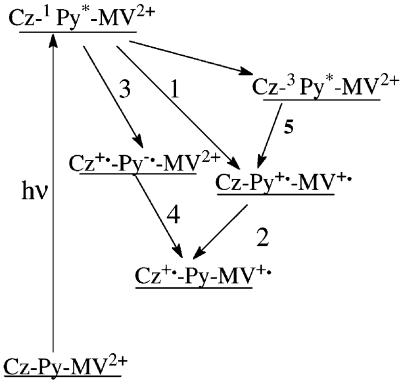

Scheme 2.

Since the efficiency of the intersystem crossing from the singlet excited Py to its triplet state is not negligible ($\Phi_{isc} = 0.38$), we also examined the possibility of the electron transfer from triplet Py to MV^{2+} (process 5 in Scheme 2) and from Cz to triplet Py. Assuming the energy of the triplet Py being ca. 48.1 kcal/mol [37], the value of ΔG involved in the former process was calculated by Eq. (2) to be ca. −13.3 kcal/mol, and that for the latter process ca. 19.7 kcal/mol. Thus, electron transfer from triplet Py to MV^{2+}(process 5) is possible, while that from Cz to triplet Py is not.

3.3. Photoelectrochemical behavior

The evidence for the long-lived charge separation based on the photochemical study is further strengthened by the photoelectrochemical measurements. We have used the L–B films described in the Section 3.2 to constitute a photoresponsive device. The L–B films of Py–MV^{2+} with SA, or the mixture of Py–MV^{2+} and Cz–MV^{2+} with SA were transferred onto an ITO glass to fabricate the electrode. The photovoltage measurements were conducted with a saturated calomel reference electrode in H_2Q aqueous solution. Irradiation was performed with the light of $\lambda > 300$ nm (light intensity 218 mW/cm^2) from the ITO electrode side, and a high photovoltage was detected. Fig. 3

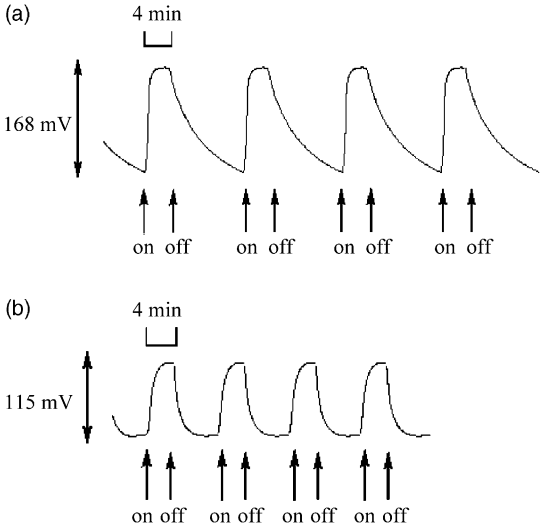

Fig. 3. Photovoltage changes induced by switching on and off the irradiation: (a) Cz–Py–MV^{2+} ITO electrode; (b) Py–MV^{2+} ITO electrode. Light intensity: 218 mW/cm^2.

gives the photovoltage changes induced by switching on and off the irradiation for Py–MV^{2+} ITO electrode and for Cz–Py–MV^{2+} ITO electrode in 36 mM H_2Q solution. Evidently, irradiation of the pyrenyl group results in the photovoltage, and the rise and decay of the photovoltage can take place repeatedly by switching the irradiation on and off. This photovoltage originates from the formation of the charge separation state $Py^{\bullet+}$–$MV^{\bullet+}$ for Py–MV^{2+} ITO electrode and $Cz^{\bullet+}$–Py–$MV^{\bullet+}$ for Cz–Py–MV^{2+} ITO electrode, and the subsequent charge transfer between $Py^{\bullet+}$ or $Cz^{\bullet+}$ and H_2Q at the interface between the electrode and the solution. As a result, the negative charge is in the ITO electrode and the positive charge in the solution. Inspection of Fig. 3 reveals that by switching on the irradiation the photovoltage is immediately produced and increases rapidly to a saturated value (ca. 115 mV for Py–MV^{2+} ITO, and ca. 168 mV for Cz–Py–MV^{2+} ITO), while the photovoltage decay is relatively slow when the irradiation is switched off. The difference in the rise and decay rates of the photovoltage is probably due to the fast forward electron transfer and the slow charge recombination as demonstrated in the Section 3.2. As shown in Fig. 3, under identical irradiation condition the photovoltage for Cz–Py–MV^{2+} ITO is ca. 1.5 times greater than that for Py–MV^{2+} ITO. This significant enhancement of the photoresponsibility is attributed to the longer-lived charge separation for the D–S–A system compared with S–A system. Although these measurements were not optimized, the photovoltage could reach 168 mV.

The photocurrent experiments also demonstrated the enhancement of the charge separation in Cz–Py–MV^{2+} system compared with Py–MV^{2+} system. These measurements employed a platinum counter electrode. The working electrode, either a Py–MV^{2+} ITO or a Cz–Py–MV^{2+} ITO, and the counter electrode were placed in a 36 mM H_2Q aqueous solution (containing 0.1 M KCl) to construct a photogalvanic cell. Irradiation was performed with light $\lambda > 300$ nm through the ITO working electrode. Anodic photocurrent with respect to the working electrode was detected during irradiation. Fig. 4 shows the current changes induced by switching on and off the irradiation. Evidently, the photoinduced forward electron transfer leads to the formation of the charge-separated state, $Py^{\bullet+}$–$MV^{\bullet+}$ for Py–MV^{2+} ITO and $Cz^{\bullet+}$–Py–$MV^{\bullet+}$ for Cz–Py–MV^{2+} ITO electrode. The generated cation radical $Py^{\bullet+}$ or $Cz^{\bullet+}$ obtains an electron from H_2Q at the electrode–solution interface, resulting in the regeneration of Py or Cz and formation of $H_2Q^{\bullet+}$. Subsequently, $H_2Q^{\bullet+}$ diffuses through the bulk solution toward the counter electrode, where it is reduced electrochemically to H_2Q. On the other hand, the reduced species $MV^{\bullet+}$ on the working electrode is oxidized back to MV^{2+} by giving an electron to the ITO electrode. Thus, there is no net chemical change associated with the function of the cell that converts light into electricity. We found that the operation time of such a photogalvanic cell might be very long. For example, we once continuously irradiated the cell for 20 h and no change in the anodic photocurrent was detected. The

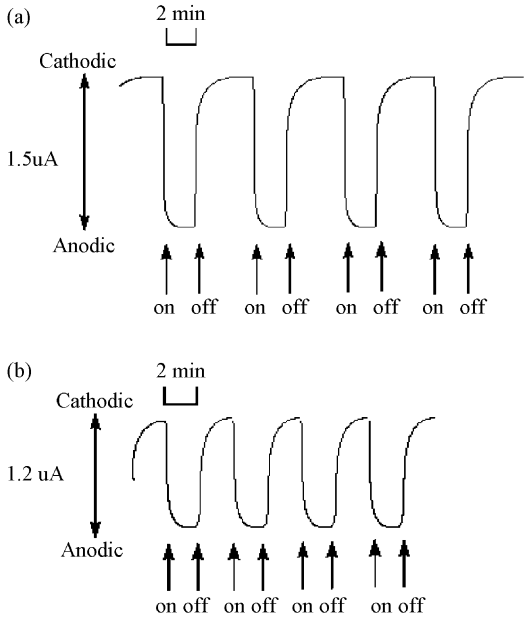

Fig. 4. Photocurrent changes induced by switching on and off the irradiation: (a) Cz–Py–MV^{2+} ITO as the working electrode; (b) Py–MV^{2+} ITO as the working electrode.

combination of photochemical and electrochemical reactions described above has been well established at semiconductor electrodes coated with L–B film [38,39] or polymer membrane [40,41] containing photoreaction components. As indicated in Fig. 4, without optimization the photoinduced currents can reach ca. 1.2 uA/cm^2 for Py–MV^{2+} ITO and 1.5 uA/cm^2 for Cz–Py–MV^{2+} ITO under a 0.2 V bias voltage. The enhancement of the current for the Cz–Py–MV^{2+} system compared with Py–MV^{2+} system, again, is attributed to the longer-lived charge separation in the former electrode.

4. Conclusion

Diazacrown ethers appending two pyrenyl or two carbazolyl groups form 1:1 host–guest complexes with methyl viologen. These complexes can act as building blocks to assemble well-organized monolayers by L–B technique. The system produced by thus synthetically simple way involves the general structure of donor–sensitizer–acceptor (D–S–A) in space, in which there are no covalent bonds between any of the photo- or redox-active components. The short distance between carbazolyl and pyrenyl, and between pyrenyl and MV^{2+} leads to fast forward electron transfer, while the spatial separation of the generated charge pair in $Cz^{\bullet+}$–Py–$MV^{\bullet+}$ inhibits the charge recombination. Thus, an exceeding long-lived (up to hours) charge separation pair was achieved. A photoelectrochemical cell constructed on the basis of the above system displays the function of conversion of light to electricity. Irradiation of a Cz–Py–MV^{2+}

film-coated ITO electrode in a H_2Q aqueous solution by visible light with intensity of ca. 218 mW/cm^2 results in a ca. 168 mV photovoltage and 1.5 uA/cm^2 photocurrent, although the measurement condition are not optimized. Furthermore, this photoelectrochemical cell operates in a regeneration mode: H_2Q is oxidized to $H_2Q^{\bullet+}$ at the interface between the solution and the irradiated L–B film ITO electrode, and the generated $H_2Q^{\bullet+}$ is reduced back to its original state at the counter electrode; MV^{2+} is reduced to $MV^{\bullet+}$ via photoinduced electron transfer, and the generated $MV^{\bullet+}$ is oxidized back to its original state by giving an electron to the ITO electrode.

Acknowledgements

We thank the National Science Foundation of China, the Ministry of Science and Technology of China (Grant Nos. G2000078104 and G2000077502) for financial support.

Appendix A. Supporting Information

Syntheses of Cz–C and Py–C, and their IR, ^{1}H-NMR and mass spectral data. See any current masthead page for ordering information and web access instructions.

A.1. Preparation of Cz–C and Py–C

Cz–C and Py–C were synthesized by substitution reaction of 4,13-diaza-18-crown-6 with *N*-(10-bromodecyl)carbazole and 1-(4-bromobutoxymethyl)pyrene, respectively. The products were isolated by column chromatograph with mixed solvents of acetone and triethylamine (95:5 in vol.%) as eluent. Recrystallization from ethanol–chloroform (20:1 in vol.%) yielded pure products. The characteristic data of Cz–C and Py–C are shown as following.

Cz–C: white powder, yield: 42%, m.p. 82–84 °C. IR (KBr) ν: 3045, 2931, 2854, 1626, 1596, 1459, 1348, 1325, 1245, 1120, 1062, 746 and 720 cm^{-1}. ^{1}H NMR ($CDCl_3$) δ: 1.2–1.5 (m, 24H), 1.6–2.0 (m, 8H), 3.1–4.0 (m, 28H), 4.3 (t, 4H), 7.1–7.3 (m, 4H), 7.3–7.5 (m, 8H), 8.1 (m, 4H). MS (FAB) *m*/*z* (%): 873 ($[M+H]^+$, 64), 449 (5), 361 (8), 335 (10), 194 (18), 180 (100), 168 (21), 100 (23), 55 (52), 44 (48). Anal. calcd. for $C_{56}H_{80}N_4O_4$: C 77.06, H 9.17, N 6.42; found C 76.97, H 9.15, N 6.29.

Py–C: pale yellow crystal, yield 60%, m.p. 106–107 °C. IR (KBr) ν: 3036, 2941, 2861, 2802, 1643, 1585, 1475, 1453, 1355, 1300, 1250, 1122, 1090, 842, 755, and 707 cm^{-1}. ^{1}H NMR ($CDCl_3$) δ: 1.6–1.7 (m, 4H), 1.75–1.85 (m, 4H), 2.8–3.3 (m, 24H), 3.4–3.5 (m, 4H), 3.55–3.75 (m, 4H), 5.19 (d, 4H), 7.95–8.40 (m, 18H). MS (FAB) *m*/*z* (%): 835($[M+1]^+$,11), 603 (3), 231 (10), 215 (100). Anal. calcd. for $C_{54}H_{62}N_2O_6$: C 77.7, H 7.43, N 3.36; found C 77.40, H 7.56, N 3.26.

References

[1] M.A. Fox, M. Chanon (Eds.), Photoinduced Electron Transfer, Vols. A–D, Elsevier, Amsterdam, 1988.
[2] J. Mattay (Ed.), Photoinduced electron transfer I–V, Topics in Current Chemistry, Vols. 156, 158, 159, 163 and 168, Springer, Berlin, 1990–1993.
[3] K.S. Schanze, K.A. Walters, Photoinduced electron transfer in metal-organic dyads, in: V. Ramamurthy, K.S. Schanze (Eds.), Molecular and Supramolecular Photochemistry, Vol. 2: Organic and Inorganic Photochemistry, Marcel Dekker, New York, 1998, pp. 75–127.
[4] T. Klumpp, M. Linsenmann, S.L. Larson, B.R. Limoges, D. Bürssner, E.B. Krissinel, C.M. Elliott, U.E.J. Steiner, Am. Chem. Soc. 121 (1999) 1076.
[5] D.M. Kaschak, J.T. Lean, C.C. Waraksa, G.B. Saupe, H. Usami, T.E.J. Mallouk, J. Am. Chem. Soc. 121 (199) 3435.
[6] D. Gust, T.A. Moore, A.L. Moore, Acc. Chem. Res. 26 (1993) 198.
[7] D. Gust, T.A. Moore, A.L. Moore, S.J. Lee, E. Bittersman, D.K. Juttrull, A.A. Rehms, J.M. DeGraziano, X.C. Ma, F. Gao, R.E. Belford, T.T. Trier, Science 248 (1990) 199.
[8] D. Gust, T.A. Moore, A.L. Moore, A.N. MacPherson, A. Lopez, J.M. DeGraziano, I. Gouni, E. Bittersman, G.R. Seely, F. Gao, R.A. Nieman, X.C. Ma, L. Demanche, S.-C. Hung, D.K. Luttrull, S.-J. Lee, P.K. Kerrigan, J. Am. Chem. Soc. 115 (1993) 11141.
[9] M.R. Wasielewski, Chem. Rev. 92 (1992) 435.
[10] P. Bonhôte, J.-E. Moser, H.-B. Robin, N. Vlachopoulos, S.M. Zakeeruddin, L. Walder, M. Grätzel, J. Am. Chem. Soc. 121 (1999) 1324.
[11] U. Bach, Y. Tachibana, J.-E. Moser, S.A. Haque, J.R. Durrant, M. Grätzel, D.R. Klug, J. Am. Chem. Soc. 121 (1999) 7445.
[12] R.D. Fossym, M.A. Fox, J. Am. Chem. Soc. 119 (1997) 1197.
[13] L.N. Dupray, M. Devenney, D.R. Striplin, T.J. Meyer, J. Am. Chem. Soc. 119 (1997) 10243.
[14] C.A. Slate, D.R. Striplin, J.A. Moss, P. Chen, B.W. Erickson, T.J. Meyer, J. Am. Chem. Soc. 120 (1998) 4885.
[15] V. Balzani, S. Campana, G. Denti, A. Juris, S. Serroni, M. Venturi, Acc. Chem. Res. 31 (1998) 26.
[16] G.M. Stewart, M.A. Fox, J. Am. Chem. Soc. 118 (1996) 4354.
[17] A. Slama-Schwok, D. Avnir, M. Ottilenghi, Nature 355 (1992) 240.
[18] T.S. Ahmadi, Z.L. Wang, T.C. Green, A. Henglein, M.A. El-Sayed, Science 272 (1996) 1924.
[19] M. Sykora, K. Maruszewski, S.M. Treffert-Ziemelis, J.R. Kincad, J. Am. Chem. Soc. 120 (1998) 3490.
[20] L. Brancaleon, D. Brousmiche, V.J. Rao, L.J. Johnston, V. Ramamurthy, J. Am. Chem. Soc. 120 (1998) 4926.
[21] C.J. Pederson, J. Am. Chem. Soc. 89 (1967) 7017.
[22] C.D. Gutsche, M. Iqbal, I. Alam, J. Am. Chem. Soc. 109 (1987) 4314.
[23] B. Dietrich, J.M. Lehn, Tetrahedron 29 (1973) 1629.
[24] J.F. Stoddart, Pure Appl. Chem. 60 (4) (1988) 467.
[25] B.L. Allwood, N. Spencer, S.-Z. Hooshang, J.F. Stoddart, D.J. Williams, J. Chem. Soc., Chem. Commun. (1987) 1064.
[26] P.R. Ashton, A.M.Z. Slawin, N. Spencer, J.F. Stoddart, D.J. Williams, J. Chem. Soc., Chem. Commun. (1987) 1066.
[27] D. Rehm, A. Weller, Isr. J. Chem. 8 (1970) 259.
[28] A.Z. Weller, Phys. Chem. 76 (1972) 3132.
[29] Y. Zhu, G.B. Schuster, J. Am. Chem. Soc. 115 (1993) 2190.
[30] C.-H. Tung, L.-P. Zhang, Y. Li, H. Cao, Y. Tanimoto, J. Am. Chem. Soc. 119 (1997) 5348.
[31] G.J. Kavarnos, N.J. Turro, Chem. Rev. 86 (1986) 401.
[32] S.L. Murvo, Handbook of Photochemistry, Marcel Dekker, New York, 1973.
[33] X.-Y. Yi, L.-Z. Wu, C.-H. Tung, J. Phys. Chem. B 104 (40) (2000) 9468.
[34] M. Borja, P.K. Dutta, Nature 362 (1993) 43.

[35] Q.H. Wu, B.W. Zhang, Y.F. Ming, Y. Cao, J. Photochem. Photobiol. A 61 (1991) 53.
[36] R.O. Loutfy, J.H. Sharp, Photogr. Sci. Eng. 20 (1976) 165.
[37] J.B. Berlman, Handbook of Fluorescence Spectra of Aromatic Molecules, Academic Press, New York, 1971.
[38] H.-X. Luo, N.-Q. Li, J. Phys. Chem. B 103 (1999) 4377.
[39] D.-G. Wu, C.-H. Huang, L.-B. Gan, J. Zheng, Y.-Y. Huang, W. Zhang, Langmuir 15 (1999) 7276.
[40] R.-J. Lin, M. Kaneko, in: K. Sienicki (Ed.), Molecular Electronics and Molecular Electronic Devices, CRC Press, Boca Raton, FL, 1992.
[41] J. Kiwi, N. Denisov, V. Nadtochenko, J. Phys. Chem. B 103 (1999) 9141.